Fish and Shellfish Immunology 91 (2019) 275–283

Contents lists available at ScienceDirect

Fish and Shellfish Immunology

journal homepage: www.elsevier.com/locate/fsi

Full length article

Glycogen phosphorylase of shrimp (*Litopenaeus vannamei*): Structure, expression and anti-WSSV function

Yong-Sheng Zhang, Fei-Xiang Li, Cui-Luan Yao*

Fisheries College, Jimei University, Xiamen, 361021, China

ARTICLE INFO

Keywords:
GP
Litopenaeus vannamei
WSSV
RNAi

ABSTRACT

Glycogen phosphorylase (GP, EC 2.4.1.1) catalyze the rate-limiting step in glycogenolysis in animals, forming glucose-1-phosphate from the terminal alpha-1,4-glycosidic bond. Therefore, GP plays a crucial role in carbohydrate metabolism. In the present study, the full-length cDNA sequence of GP (*Lv*GP) was cloned from shrimp, *Litopenaeus vannamei*. The obtained 3242-bp *Lv*GP cDNA sequence included a 5′-terminal untranslated region (UTR) of 48 bp, an open reading frame (ORF) of 2559 bp encoding a polypeptide of 852 amino acids (aa) and a 3′-UTR of 635 bp. The predicted *Lv*GP protein sequence contained a typical phosphorylase domain (113–829 aa) and shared 72%–97% identities with GP from other species. Phylogenetic analysis revealed that *Lv*GP showed the closest relationship with GP from *Marsupenaeus japonicus*. Tissue expression profiles showed that *Lv*GP existed in most examined tissues, with the most predominant expression in the brain, followed by the muscles and stomach. *Lv*GP transcripts in hepatopancreas and hemocytes were up regulated after the WSSV challenge. Furthermore, the role of *Lv*GP in shrimp defending against WSSV infection was investigated by RNA interference (RNAi). Our findings showed that WSSV proliferation and shrimp accumulative mortality increased significantly after *Lv*GP RNAi ($P < 0.01$). The glycogen, glucose, and pyruvate content decreased in GP RNAi shrimp after WSSV injection, however, the lactate and ATP concentration enhanced. Moreover, lectin and anti-lipopolysaccharide factor2 (ALF2) were induced in *Lv*GP silencing shrimp after WSSV infection, whereas the expression levels of crustin, ALF1 and ALF3 decreased. Our results suggested that the *Lv*GP might play a crucial role in shrimp defending against WSSV infection by regulating metabolism and affecting the anti-infectious gene expression.

1. Introduction

The commercial shrimp, *Litopenaeus vannamei* farming industry is threatened by many pathogens throughout the world. Among them, white spot syndrome virus (WSSV) is one of the most virulent and has caused a huge economic loss. However, shrimp lack acquired immunity, instead they have developed an innate immune system to defend against pathogenic infections.

Previous studies demonstrated that many energy metabolic enzymes showed a close relationship with shrimp immune response [1–3]. Recent studies showed that a large amount of energy might be required during WSSV infection and replication [4]. On the other hand, in order to maximize the efficiency of their replication, many viruses might escape the immunologic surveillance through interfering with the normal metabolic functions of the host [5].

As the primary energy sources, carbohydrates might play an important role in maintaining physiological homeostasis in crustaceans. It was demonstrated that pathogenic challenge could impose high energetic costs for immune regulation. And carbohydrate metabolism including glucose degradation, glycogenolysis, and gluconeogenesis were assumed to enhance to accommodate these increased energy requirements [6].

Glycogen phosphorylase (GP) catalyzes the rate-limiting step in glycogenolysis in animals by releasing glucose-1-phosphate(G1P) from the terminal alpha-1,4-glycosidic bond [7], and G1P can enter into the glycolytic pathway and tricarboxylic acid (TCA) cycle by forming pyruvate/lactate or enter into the pentose phosphate pathway (PPP) through glucose-6-phosphate (G6P) and is involved in nucleic acid metabolism by generating nucleotides and NADPH [8]. It was reported that the GP depletion in cancer cells led to glucose metabolism disorders and affected the NADPH level of PPP, which might have changed gene expression and strongly inhibited tumor growth [8]. In vertebrates, glycogen is mainly found in the liver and skeletal muscle where it constitutes stores of readily available glucose to supply to tissues [9].

* Corresponding author:
E-mail address: clyao@jmu.edu.cn (C.-L. Yao).

https://doi.org/10.1016/j.fsi.2019.05.043
Received 3 April 2019; Received in revised form 14 May 2019; Accepted 20 May 2019
Available online 21 May 2019

The imbalance of glucose metabolism might result in the energy production and many other physiological disorders [10]. Shrimp consume a large amount of energy to maintain normal biological events, and increased energy requirements were also detected in shrimp after WSSV infection [1–3,11,12]. However, as a crucial enzyme in metabolism, the cDNA sequence of GP in crustaceans was only identified in kuruma shrimp, *Marsupenaeus japonicus* [13], and brown shrimp *Artemia sinica* [14] up to the present study. It was shown that GP might be involved in development and response to hormone stimulation and environmental stress in crustaceans [13,14]. However, little is known in regards to the role of GP in shrimp immune response [15,16].

In the present study, the full-length cDNA sequence of *Lv*GP was cloned from shrimp, *L. vannamei*, and the expression characterizations were investigated in hemocytes and hepatopancreas. Furthermore, the role of *Lv*GP in shrimp defending against WSSV infection was studied by using RNAi approach, and the related metabolic molecules and immune factors were also investigated, aiming at better understanding the function of GP in shrimp anti-WSSV immune response.

2. Materials and methods

2.1. Experimental animals

Juvenile shrimp *L. vannamei* (length 6.70 ± 2.40 cm, weight 2.80 ± 1.20 g) were obtained from Longcheng Shrimp Farm in Xiamen, China. These shrimp were acclimated in recirculating tanks filled with air-pumped seawater with a salinity of 20 practical salinity units (psu) at 26 ± 1 °C for 7 days and were fed with commercial food pellets two times per day. WSSV was kindly presented by Dr. Feng Yang at the Third Institute of Oceanography, China. Shrimp infection was performed by intramuscular injection of 20 μL with 1.0×10^7 WSSV viral particles in the penultimate abdominal segment according to our previous report [17]. Shrimp were injected with the same volume of PBS (140 mM NaCl, 3 mM KCl, 8 mMNa_2HPO_4, 1.5 mM KH_2PO_4, pH 7.4) as control. The hemocytes and hepatopancreas pooled from five shrimp were sampled at 6, 12, 24, 48 and 96 h after injection respectively, and every treatment consisted of three replicates (N = 3). Hemolymph was extracted from the ventral sinus of shrimp and diluted 1:2 in precooled sterile shrimp anti-coagulant as our previous described [18]. Hemocytes were separated by centrifugation at 800 *g* for 5 min at 4 °C and immediately put into liquid nitrogen for frozen storage. Meanwhile, heart, ventral nerve cord, muscle, stomach, brain, intestine, gill and hepatopancreas were dissected. After centrifugation or dissection, all samples were frozen immediately in liquid nitrogen and stored at −80 °C for RNA and DNA extraction.

2.2. Total RNA extraction and cDNA preparation

Total RNA was extracted from different tissues of shrimp using the Eastep® Super Total RNA Extraction Kit (Promega, USA) according to the manufacturer's instructions. Then total RNA was used to synthesize first strand cDNA with a PrimeScript® 1st Strand cDNA Synthesis Kit (TAKARA, Japan) following the manufacturer's protocol. The cDNA was then stored at −20 °C until used in real-time quantitative reverse transcription PCR (qPCR) and double-stranded RNA (dsRNA) synthesis.

2.3. Full-length cDNA cloning of LvGP

The open reading frame (ORF) sequence of *Lv*GP was obtained by nested PCR amplification with four gene specific primers *Lv*GP-F1/*Lv*GP-R1 and *Lv*GP-F2/*Lv*GP-R2 (Table 1). The 3′ and 5′ ends were obtained by rapid amplification of cDNA ends (RACE) approaches. The 3′ end PCR of the *Lv*GP gene was performed with a mixed cDNA template from multiple tissues using the gene-specific primer GP3′-1 and adapter primer AOLP, and GP3′-2 and AP (Table 1) by nest PCR at an annealing temperature of 49 °C and 60 °C, respectively. For the 5′ end, the hepatopancreas mRNA was transcribed by M-MLV reversed transcriptase with Oligo$(dT)_{18}$ primer and then purified with a DNA purification kit (TAKARA, Japan) and tailed with poly(C) according to the manufacture's protocol. The 5′ end PCR of the *Lv*GP gene was performed using the gene-specific primer GP5′-1 and adapter primer AAP and GP5′-2 and AP (Table 1) by nest PCR at an annealing temperature of 55 °C and 58 °C, respectively. All PCR products were gel-purified, ligated into PMD19-T vector and transformed into the competent *Escherichia coli* TOP10 cells. Positive clones containing the expected-size inserts were screened by colony PCR and then sequenced by Borui Biotechnology Company (Xiamen, China).

2.4. Sequence analysis and phylogenetic tree construction

The gene sequence was analyzed by the online program ExPASy (http://www.au.expasy.org/) and BLAST (http://blast.ncbi.nlm.nih.gov/). The deduced amino acid sequence was analyzed with the Expert Protein Analysis System (ExPASy) (http://www.au.expasy.org). Multiple sequence alignments were performed using the ClustalW (http://www.ebi.ac.uk/tools/msa/clustalw2). The protein domain was predicted by Simple Modular Architecture Reach Tool (SMART) (http://smart.embl-heidelberg.de). The phylogenetic tree based on multiple protein alignments was constructed using the neighbor-joining (NJ) method by MEGA7.0 software; the sequences used for phylogenetic analysis were shown in Table 2. The deduced amino acid sequences of GP from other invertebrates, fish, amphibian, birds and mammals were used in the analysis (Table 2). Bootstrap sampling was reiterated 1,000 times.

2.5. LvGP tissue expression analysis

QPCR was used to analyze the expression of *Lv*GP in different tissues of normal shrimp. The transcriptional levels of *Lv*GP were detected with the primers qGP-F and qGP-R (Table 1). β-actin was employed as the internal reference gene with primers β-actin-F/β-actin-R (Table 1). The qPCR reaction was carried out in a total volume of 20 μL, containing 10.2 μL GoTaq®qPCR Master Mix (SYBR Green) (Promega, USA), 0.5 mM forward primer, 0.5 mM reverse primer, 1 μL cDNA template and 7.8 μL RNase free water. The program was set as the following: 95 °C for 2 min; 40 cycles of 95 °C for 15 s, annealing temperature of 60 °C for 1 min and 72 °C for 20 s. $2^{-\Delta\Delta CT}$ method was employed to calculate the relative expression level of the target gene [19]. The expression levels of *Lv*GP in hepatopancreas and hemocytes during WSSV challenge were performed following the same method. An independent sample *t*-test was used to analyze the differences among samples by SPSS 18.0. $P < 0.05$ was considered statistically significant.

2.6. RNAi experiment

2.6.1. Synthesis of double-stranded RNA

The synthesis of a 440-bp double-strand RNA (dsRNA) of *Lv*GP (ds*Lv*GP) was performed with two pair of primers GP-IF1/GP-IR1 and GP-IF2/GP-IR2 contained T7 promoter sequences (Table 1). The PCR was conducted as follows: denaturation at 94 °C for 5 min; 40 cycles of 94 °C for 30 s, 60 °C for 30 s, 72 °C for 30 s. Then the PCR products were purified and used as the templates for dsRNA synthesis by the T7 RiboMAX™ Express RNAi System (Promega, USA). Synthesized ds*Lv*GP was quantified by a Nanodrop 2000 spectrophotometer (Thermo Fisher Scientific, USA), assessed by electrophoresis on 1% agarose gel, and stored at −80 °C. A 500-bp dsRNA fragment of enhanced green fluorescent protein (dsGFP) gene cloned with the primers GFP-IF1, GFP-IR1 and GFP-IF2 and GFP-IR2 (Table 1) from the pGFP-N1 plasmid was used as control.

The silencing efficiency of dsGP was assessed by detecting the expression level of *Lv*GP in muscle tissue of shrimp at 24 after dsRNA injection. Total RNA was extracted and cDNA reverse transcribed as

Table 1
The primers used for gene cloning and expression analysis in this study.

Primer	Sequence(5′-3′)	Tm(°C)	Application
*Lv*GP-F1	AGTGCTTGGCTGGACTGAG	55	Gene cloning
*Lv*GP-R1	GTATCCCACAGGCAAACTCT		
*Lv*GP-F2	TTGGCTGGACTGAGGTGAA	56	
*Lv*GP-R2	GTATCCCACAGGCAAACTCT		
GP3′-1	TTCTTCCTGTTCGCTGACTT	49	
GP3′-2	AGAAGTTGCCTGCTCCCCACG	60	
GP5′-1	GTTGCCAAACCGCAGCCAGTC	55	
GP5′-2	ACAAGCCGACTGAATGCCCAA	58	
AP	GGCCACGCGTCGACTAGTAC		
AOLP	GGCCACGCGTCGACTAGTACTTTTTTTTTTTTTTTT		
AAP	GGCCACGCGTCGACTAGTACGGGGGGGGGG		
qGP-F	GGGCATTCAGTCGGCTTGTG	60	Transcripts expression
qGP-R	TTGCCAAACCGCAGCCAGTC		
β-actin-F	GAAGTAGCCGCCCTGGTTGT	60	
β-actin-R	GGATACCTCGCTTGCTCTGG		
GP-IF1	GGATCCTAATACGACTCACTATAGGCCTGATGACTGGCTGCGGTTTG	56	Synthesis of dsRNA
GP-IR1	TCCGTGCGAACCTGGTCTTTTG		
GP-IF2	GGATCCTAATACGACTCACTATAGGTCCGTGCGAACCTGGTCTTTTG	56	
GP-IR2	CCTGATGACTGGCTGCGGTTTG		
GFP-IF1	GGATCCTAATACGACTCACTATAGGACAAGTTCAGCGTGTCCG	55	
GFP-IR1	TCGCCGATGGGGGTGTTC		
GFP-IF2	ACAAGTTCAGCGTGTCCG	55	
GFP-IR2	GGATCCTAATACGACTCACTATAGGTCGCCGATGGGGGTGTTC		
VP28-F	TTCTTTCACTCTTTCGGTCGT	54	Virus replication detection
VP28-R	GCCAACTTCATCCTCATCAAT		
qVP28-F	ATCCGCAATGGAAAGTCTGA	58	
qVP28-R	GGGTGAAGGAGGAGGTGTT		
qLectin-F	TCAGAACTGCCTTGCGATCAC	60	Immune factors expression
qLectin-R	CACGCCATTTGCTCATCCA		
qCrustin-F	GGAGGGTCAAGCCTACTGC	60	
qCrustin-R	ACGTGGGCATGTGGGAC		
qALF1-F	GGATGTGGTGTCCTGGATGG	60	
qALF1-R	GCGTCGTCCTCCGTGATG		
qALF2-F	GCGAACAAACTCACTGGACTG	60	
qALF2-R	ACATGCGACCCTGGAATACAG		
qALF3-F	GACCTGTCCAACCCTGAGC	60	
qALF3-R	TCGCCTCCTCCTCCGTTATC		

Table 2
Predicted protein sequences of GP used for multiple sequence alignments and phylogenetic analysis.

Spieces	Common name	Database Acc NO.	Identity(%)
Marsupenaeus japonicus	Kuruma prawn	GenBank: BAJ23879	97%
Daphnia magna	Water flea	GenBank: JAN85876	82%
Drosophila melanogaster	Fruit fly	GenBank: AAD27759	79%
Artemia sinica	Artemia salina	GenBank: AFK10487	79%
Mus musculus	Mouse	GenBank: AF288783	73%
Homo sapiens	Human	GenBank: AAC18079	73%
Anopheles darlingi	Mosquitoes	GenBank: ETN62232	81%
Danio rerio	Zebrafish	GenBank: AY576991	75%
Crassostrea gigas	Pacific oyster	GenBank: AY496065	74%
Oryctolagus cuniculus	Rabbit	GenBank: D00040	75%
Harmonia axyridis	Ladybug	GenBank: KX766454	80%
Ostrinia furnacalis	Asian corn borer	GenBank: JX113672	78%
Gallus gallus	Chicken	GenBank: AY271349	74%
Bombyx mori	Silkworm	GenBank: EU527367	77%
Spodoptera exigua	Beet armyworm	GenBank: FJ754277	77%
Ascidia sydneiensis samea	Sea squirts	GenBank: AB212671	72%

above. β-actin was used as internal control.

2.6.2. WSSV challenge in LvGP RNAi shrimp

To investigate the function of *Lv*GP in WSSV infection, each juvenile shrimp was intramuscularly injected with 3 μg/g shrimp of dsGP dissolved in PBS, and 1.0×10^7 copies of WSSV were injected into each shrimp at 24 h after ds*Lv*GP injection. Shrimp injected with dsGFP and PBS were set as control. The muscle tissues were dissected and sampled and pooled from 5 shrimp at 0, 24 and 48 h after WSSV injection, respectively and used for WSSV copy numbers, biochemical analysis and immune gene detection. The dead shrimp were removed and recorded immediately, and every treatment consisted of triplicates (N = 3).

2.7. Quantitative WSSV copy numbers and shrimp mortality in LvGP RNAi shrimp

The WSSV virus amplification was qualified by detecting the WSSV envelope protein 28 (VP28) expression in muscle tissue according to previous investigations [17]. Briefly, DNA was extracted from the muscles after 0 h, 24 h and 48 h dsRNA injection according to the manufacture's instruction (TIANamp, China). Absolute qPCR analysis was carried out with two WSSV specific primers qVP28-F and qVP28-R (Table 1). Then, standard curves from serial dilutions (10^1 to 10^{10}) of the 499-bp VP-28 PCR fragments were generated and used to calculate the number of WSSV copies according to Yang and colleagues [20]. WSSV reproduction was represented by the virus copy numbers per ng muscle DNA. Shrimp mortality was calculated by the numbers of dead animals in a tank of 200 *Lv*GP RNAi shrimp in 48 h after WSSV injection.

2.8. Biochemical assay

To assess the concentration of glycogen, glucose, pyruvate, lactate and ATP, the sampled hepatopancreas were homogenized with ice-cold PBS and centrifuged at 4 °C for 15 min. The supernatant was collected for biochemical assay using commercial kits (Nanjing Jiancheng Bioengineer Institute) according to the manufacture's instruction. The

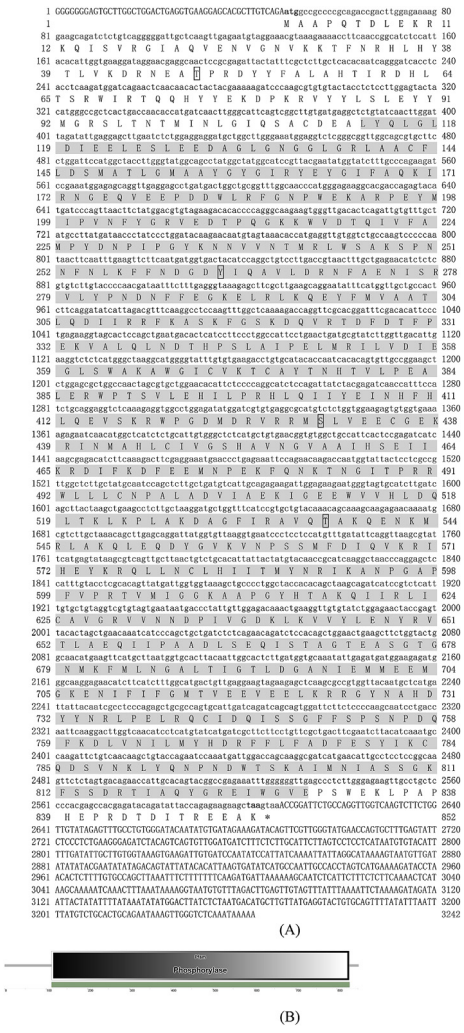

Fig. 1. The complete nucleotide and deduced amino acid sequence of *Lv*GP. (A)The ORF of the nucleotide sequence is predicted into amino acids. The start codon (ATG), and the stop codon (TAA) is indicated with bold letters. A deduced conservative phosphorylase domain (113–829 aa) is shaded. (B) The deduced conserved phosphorylase domain of *Lv*GP analyzed by SMART.

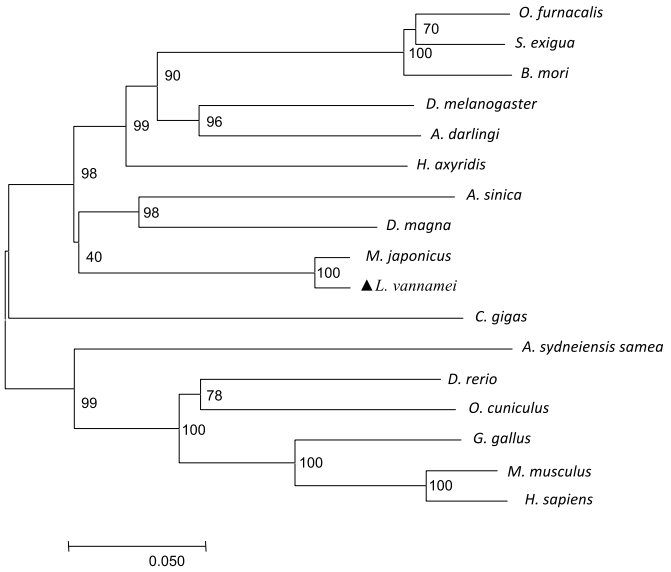

Fig. 2. Phylogenetic tree of predicted *Lv*GP protein sequences. Complete amino acid sequences were aligned by using CLUSTAL W, and the tree was constructed with NJ method in MEGA 7.0 and a bootstrap analysis was performed using 1000 replicates to test the relative support for particular clades. GenBank accession numbers of these proteins are listed in Table 2.

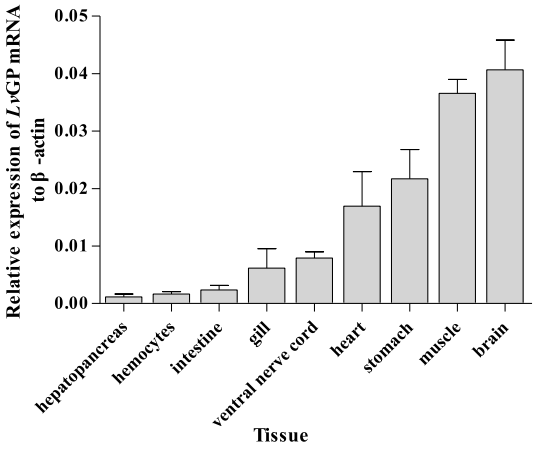

Fig. 3. The tissue distribution analysis of *Lv*GP in different tissues of shrimp by qPCR. β-actin was used as the internal control. Each bar represented the mean ± SD of three independent samples (N = 3).

protein concentration was assayed according to Bradford (1976) [21], using bovine serum albumin as standard.

2.9. Quantitative analysis of immune-related genes expression

To investigate the role of GP in shrimp defending against WSSV infection, the expression levels of some anti-WSSV immune genes including lectin, crustin, ALF1, ALF2 and ALF3 were examined in *Lv*GP RNAi shrimp after WSSV injection. Total RNA was extracted from hepatopancreas of *Lv*GP or GFP RNAi shrimp at 0 h, 24 h and 48 h after WSSV infection. The cDNA synthesized from 1 μg RNA was used as a template. Crustin, lectin, ALF1, ALF2 and ALF3 were determined by qPCR as above. The gene specific primers were used for the qPCR amplifications and β-actin as internal reference (Table 1). All data were given in terms of relative mRNA expression as means ± SE (N = 3).

2.10. Statistical analysis

The data were analyzed by one-way analysis of variance (one-way ANOVA) using PASW Statistics 18. The *P* value smaller than 0.05 was considered a statistically significant difference ($P < 0.05$). $P < 0.01$ was considered a statistically extremely significant difference. The results were plotted by Origin 8.0 software (Origin Lab Corporation, MS, USA). Asterisks and double asterisks represent statistically significant differences and extreme significant differences between experimental treatments and the control, respectively.

3. Results

3.1. Cloning and sequence analysis of LvGP

A 3242-bp nucleotide sequence representing the full-length cDNA sequence of *Lv*GP was obtained, including 2559 bp ORF encoding 852 amino acids, a 5′UTR of 48 bp and a 3′UTR of 635 bp including a polyA tail (Fig. 1A). Multiple alignments showed that *Lv*GP shared the highest identity of 97% with GP from shrimp *M. japonicus* and 72%–82% identities with GP from other species (Table 2). SMART analysis showed that *Lv*GP contained a deduced conservative phosphorylase domain (113–829 aa) in the glycosyltransferase family. Additionally, two conserved threonine residues, a conserved tyrosine residue and a typical serine residue in *Lv*GP were identified at amino acid positions of Thr^{48}, Thr^{537}, Tyr^{263} and Ser^{430} of the predicted *Lv*GP protein sequence,

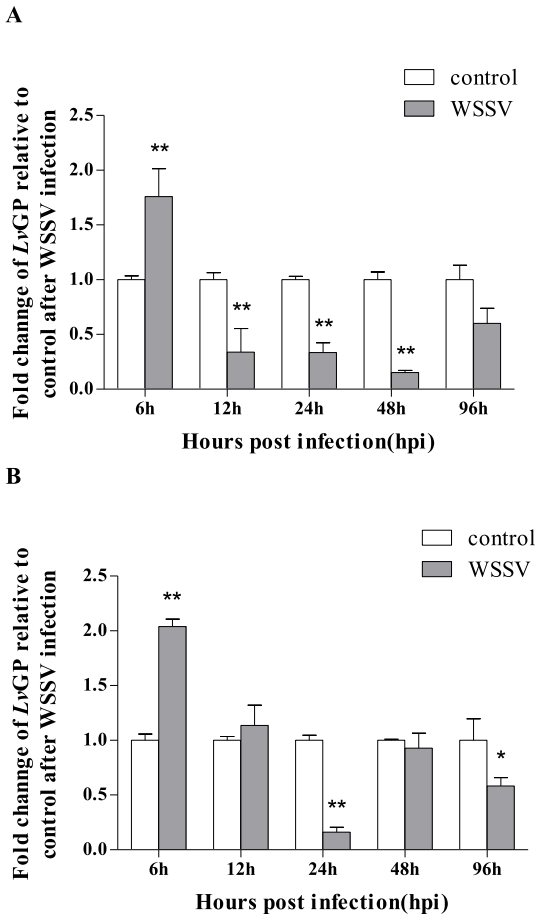

Fig. 4. QPCR analysis of *Lv*GP expression in hepatopancreas (A) and hemocytes (B) after WSSV challenge at 6, 12, 24, 48 and 96 h post-infection. Each bar represented the mean ± SD of three independent samples. Asterisk and double asterisks indicated significant difference (**$P < 0.01$,*$P < 0.05$) (N = 3).

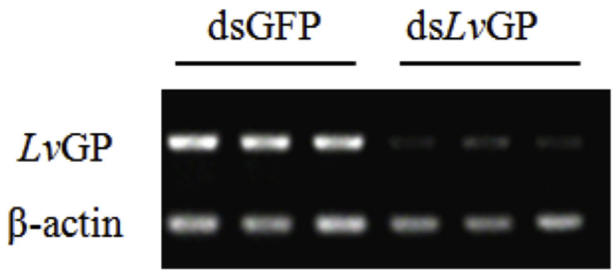

Fig. 5. Detection of *Lv*GP RNAi efficiency in muscle tissue by semi-quantitative PCR. The expression level of *Lv*GP was examined using semi-quantitative PCR to verify the silencing efficiency of RNAi. β-actin was used as the internal control. Each lane represents the result from three independent shrimp per group (N = 3).

respectively (Fig. 1B).

3.2. Phylogenetic analysis

In order to reveal the evolutionary relationship of *Lv*GP, a phylogenetic tree was constructed by using the predicted GP protein sequences form different species (Fig. 2). The results showed that *Lv*GP was clustered into a subgroup with GP from other crustaceans and showed the closest relationship with GP from *M. japonicus*. The relationships observed within this cluster reflected the taxonomic positions of the species.

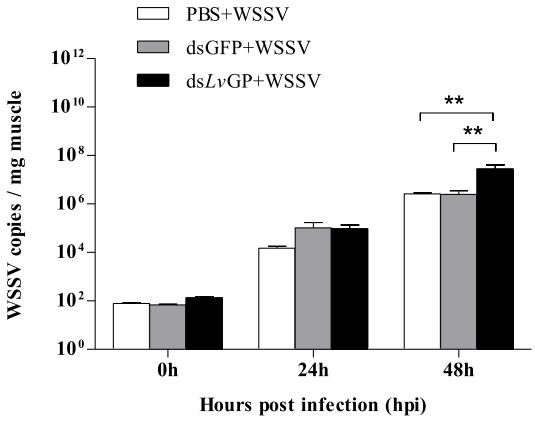

Fig. 6. Detection of WSSV copy numbers in shrimp following treatment with ds*Lv*GP. Shrimp were challenged with WSSV after 24 h ds*Lv*GP injection. Shrimp were injected with WSSV after 24 h of dsGFP and PBS injection as controls. Total DNA was extracted from shrimp muscle and used for WSSV copy numbers detection by absolute qPCR. Each bar represents the mean ± SD of three samples (*$P < 0.05$, **$P < 0.01$) (N = 3).

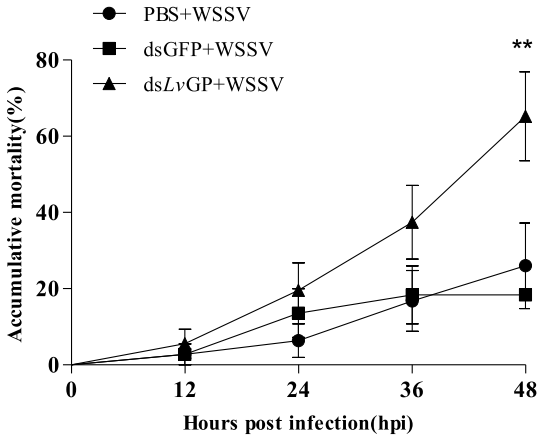

Fig. 7. Cumulative mortality of *Lv*GP RNAi shrimp in 48 h after WSSV injection. The cumulative mortality of ds*Lv*GP RNAi shrimp by counting the dead shrimp at 0, 12, 24, 36 and 48 h after WSSV injection, with dsGFP and PBS injection as control. Error bars represented ± SD of three replicates. Analyzed with the GraphPad Prism software using the Log-rank (Mantel-Cox) method. All data were given in terms of means ± SE (Standard Error) Asterisks indicated significant differences and extreme significant difference (*$P < 0.05$, **$P < 0.01$) (N = 3), respectively.

3.3. Tissue expression profile of LvGP

The constitutive expression of *Lv*GP in different tissues showed that *Lv*GP was expressed in most examined tissues, with the most predominant expression level in the brain, followed by the muscles and stomach, and expression levels of *Lv*GP in hepatopancreas, hemocytes and intestine were very weak (Fig. 3).

3.4. Expression profiles of LvGP mRNA in hepatopancreas and hemocytes after WSSV infection

*Lv*GP transcripts in hepatopancreas after WSSV infection were shown in Fig. 4A. *Lv*GP transcripts increased extremely significant at 6 h, with the peak value of 1.76-fold as much as the control ($P < 0.01$). However, it decreased significantly from 12 h to 48 h after virus injection ($P < 0.01$), with the lowest value of 15% as much as the control at 48 h, and then it returned to the control at 96 h. The transcripts of *Lv*GP in hemocytes after WSSV injection were shown in Fig. 4B. Similarly, significant up-regulation of *Lv*GP transcripts appeared at 6 h with the

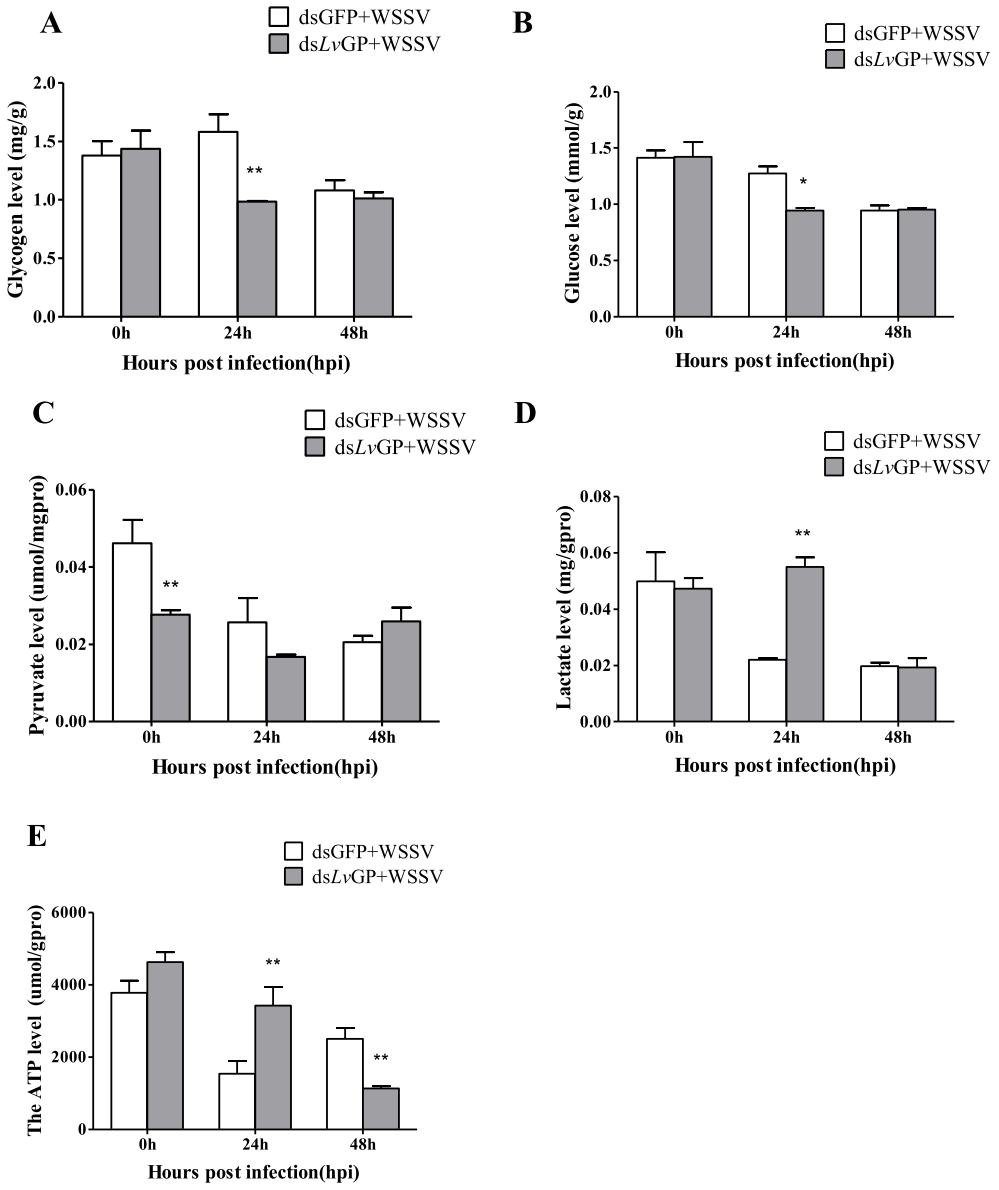

Fig. 8. The changing of the concentration of some metabolic products in hepatopancreas of *Lv*GP RNAi shrimp after WSSV injection. A. glycogen, B. glucose, C. pyruvate, D. lactate and E. ATP. WSSV was injected into the shrimp after 24 h of *Lv*GP RNAi, samples were collected at 0, 24 and 48 h WSSV post-infection (hpi). Statistical significance between *Lv*GP RNAi groups and their GFP RNAi controls were indicated by single or double asterisks. Single asterisk and double asterisks indicated significant difference (*$P < 0.05$) and extreme significant difference (**$P < 0.01$) (N = 3).

peak value of 2.04-fold as much as the control ($P < 0.01$), and then it showed fluctuation as it decreased from 12 to 96 h, with the lowest value of 16% as much as the control appearing at 24 h ($P < 0.01$).

3.5. Cumulative mortality and WSSV proliferation after LvGP knockdown

The optimal injection amount of dsRNA for *Lv*GP RNAi was 3 μg/g shrimp, and the negative *Lv*GP expression maintained up to 24 h after dsRNA injection (Fig. 5).

WSSV amplification in *Lv*GP RNAi shrimp was shown in Fig. 6. The results showed that WSSV copy numbers increased gradually after injection. However, compared with dsGFP RNAi and PBS controls, significant high copy numbers of WSSV appeared at 48 h ($P < 0.01$) in *Lv*GP RNAi group, with values 11.21 times as much as the GFP RNAi control and 10.77 times as much as the PBS control. No significant difference of WSSV replication was detected between the GFP RNAi control group and the PBS control group.

Cumulative mortality of *Lv*GP RNAi shrimp after WSSV injection was shown in Fig. 7. The cumulative mortality of shrimp increased gradually after the WSSV challenge, with the lowest value of 5% mortality appearing at 12 h and the greatest value of 65% mortality at 48 h after WSSV injection, which was significantly higher than those in the control shrimp (26% in the PBS control and 18% in the GFP RNAi control).

3.6. Biochemical analysis

The concentration of some important metabolic products in hepatopancreas of *Lv*GP RNAi shrimp after WSSV injection were shown in Fig. 8. Compared with GFP RNAi control, the glycogen concentration decreased significantly in *Lv*GP RNAi group at 24 h after WSSV injection, with the lowest value approximating 68% as much as the control ($P < 0.01$). However, it recovered to the control level at 48 h after WSSV injection (Fig. 8A). The changing of glucose concentration showed a similar profile with that of glycogen concentration, with the lowest level at 24 h as much as 66% of the GFP RNAi control

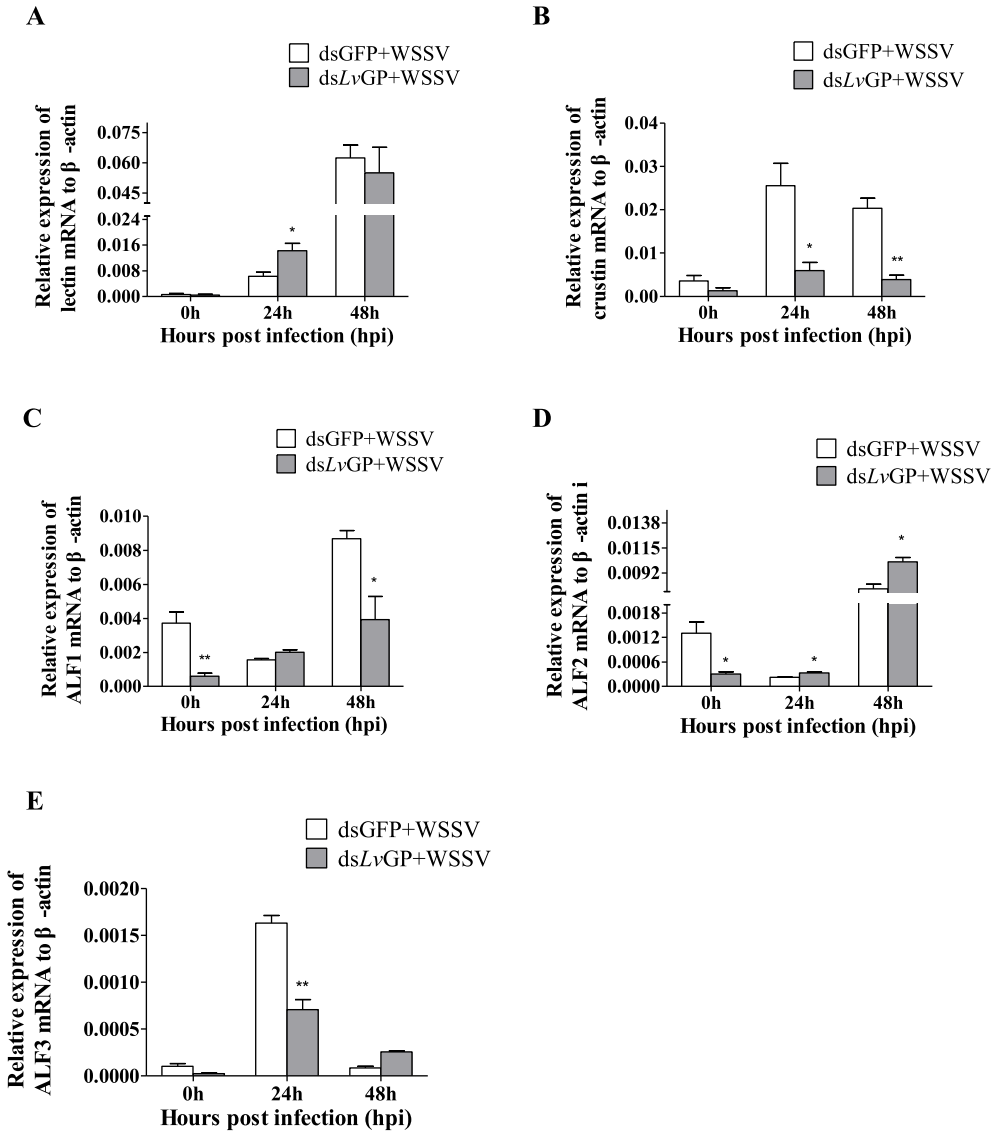

Fig. 9. The expression levels of some anti-WSSV genes in hepatopancreas of *Lv*GP knockdown shrimp after WSSV infection. A. Lectin; B. Crustin; C. ALF1; D. ALF2 and E. ALF3. WSSV was injected into the shrimp after 24 h of *Lv*GP RNAi, samples were collected at 0, 24 and 48 h WSSV post-infection (hpi). Statistical significance between *Lv*GP RNAi groups and their GFP RNAi controls were indicated by single or double asterisks. Single asterisk and double asterisks indicated significant difference (*$P < 0.05$) and extreme significant difference (**$P < 0.01$) (N = 3).

($P < 0.05$) (Fig. 8B). The pyruvate levels decreased significantly at 24 h after LvGP RNAi (0 h after WSSV injection), with a value of 60% as much as the control ($P < 0.01$). However, when compared with the control group, it did not show significant difference at 24 and 48 h after WSSV injection (Fig. 8C). Compared with the control group, lactate concentration increased significantly in the *Lv*GP RNAi group at 24 h after WSSV injection, with a peak value 2.50 times greater than that of the control ($P < 0.01$). However, it returned to the control level at 48 h after injection (Fig. 8D). The ATP levels increased significantly in *Lv*GP knockdown shrimp at 24 h after WSSV injection, as they were 2.23-fold greater than that of the control; however, the levels decreased significantly and were 45% as much as the control at 48 h WSSV injection ($P < 0.01$) (Fig. 8E).

3.7. The expression of some immune genes in LvGP RNAi shrimp after WSSV infection

The expression levels of some immune genes in hepatopancreas of *Lv*GP RNAi shrimp after WSSV injection were shown in Fig. 9. Lectin transcripts up-regulated significantly at 24 h post-injection, 2.24-fold as much as the control ($P < 0.05$) (Fig. 9A). However, crustin transcripts decreased significantly from 24 to 48 h after WSSV injection, with the lowest value of 0.19-fold as much as the control appearing at 48 h ($P < 0.01$) (Fig. 9B). Significant low expression levels of ALF1 in *Lv*GP silencing group were detected at 0 h and 48 h after WSSV injection, with the lowest value of 0.16-fold as much as the control appearing at 0 h post-injection ($P < 0.01$) (Fig. 9C). ALF2 transcripts down-regulated at 0 h post-injection, with the lowest value of 0.23-fold as much as the control ($P < 0.01$). However, it increased significantly from 24 to 48 h after WSSV injection, with the peak value of 1.31-fold as much as the control appearing at 48 h ($P < 0.01$) (Fig. 9D). Compared to the control group, ALF3 decreased significantly at 24 h post-injection, with the value of 0.43-fold as much as the control ($P < 0.01$) (Fig. 9E).

4. Discussion

In the present study, a 3242-bp full-length cDNA sequence of *Lv*GP was cloned and characterized from *L. vannamei* (GenBank: MK721970) (Fig. 1). The deduced amino acid sequence of *Lv*GP shared high

identities with GP from kuruma shrimp and contained the conserved phosphorylase domain and typical amino acids Thr^{48}, Thr^{537}, Tyr^{263} and Ser^{430} for phosphorylation and activation in the GP family [22] (Table 2). Phylogenetic analysis showed that *Lv*GP clustered into the same group with GP from invertebrates shared the closest relationship with GP from *M. japonicas*, (Fig. 2), indicating a high degree of conservation of GP through evolution and that *Lv*GP might possesses similar functions to the conservative GP family.

The ubiquitous expression of *Lv*GP was detected in most examined tissues of *L. vannamei* (Fig. 3), with the predominant expression of *Lv*GP in brain and muscle tissue, indicating that *Lv*GP might play important roles in the nerve conduction and movement in shrimp *L. vannamei*. It was demonstrated that glycogen might play a crucial role in brain energy metabolism of mouse (*Mus musculus*) and the high expression levels of GP were detected in muscles and brain of zebrafish (*Danio rerio*) and Chinese mitten crab (*Eriocheir sinensis*) [22–24]. However, *Lv*GP expression was limited to the hepatopancreas and hemocytes, which is similar to that of kuruma shrimp [13]. In addition, the weak expression of GP was also detected in liver of human, salmon and hepatopancreas of oyster [25–27], suggested that the hepatopancreas and hemocytes of normal shrimp might not need to synthesize a large amount GP to maintain their activities [28,29].

It was reported that a large amount of energy might be required in shrimp immune response [4]. Therefore, the expression levels of some metabolic enzymes in shrimp could be induced after immune challenge [30,31]. Changing expression of *Lv*GP was detected in hepatopancreas and hemocytes after WSSV injection in the present study (Fig. 4A and B). *Lv*GP increased significantly in both hepatopancreas and hemocytes at 6 h after WSSV injection, which might be due to the energy requirements of immune response and virus replication [1,2]. However, the decrease of *Lv*GP might be due to metabolic disorders caused by WSSV infection. Previous investigations demonstrated that WSSV infection could trigger metabolic changes in shrimp, which supported the bioenergetic and biosynthetic requirements of viral replication [2].

To further confirm the function of *Lv*GP in shrimp defending against WSSV infection, *Lv*GP RNAi was carried out. The results showed that WSSV replication increased significantly after *Lv*GP RNAi (Fig. 6), which might result in a higher shrimp accumulative mortality after WSSV infection (Fig. 7). Some previous studies have demonstrated the acceleration of glycogen degradation, glucose utilization, and energy generation in immunocytes of shrimp after pathogenic infection [32,33]. In the present study, the decrease of glycogen, glucose and pyruvate concentration was detected in *Lv*GP RNAi shrimp after WSSV infection whereas lactate concentration increased (Fig. 8), suggesting that lactate might play an important role during *Lv*GP silencing shrimp defending against WSSV infection. This increase might be a metabolic compensation and contribute to the ATP production in the early stage of infection. However, this metabolic compensation might not be sustainable. Previous investigations demonstrated that WSSV infection caused warburg effect which resulted due to the increase of lactate synthesis and was beneficial to WSSV replication [2].

In invertebrates, crustin and lectin have been identified by recognizing double stranded RNAs or glycoproteins from viruses, and then triggering a series of antimicrobial responses [34,35]. ALFs have been proved possessing strong antiviral activities in shrimp [36]. It was demonstrated that the expression of these antimicrobial peptides could be induced by WSSV infection [37,38]. Our results showed that lectin and ALF2 transcripts could be induced significantly in *Lv*GP RNAi shrimp by WSSV injection (Fig. 9A and D), suggesting that lectin and ALF2 might play an important role in *Lv*GP silencing shrimp defending against WSSV infection. However, compared with the dsGFP control, *Lv*GP RNAi might result in the transcriptional inhibition of crustin, ALF1, and ALF3, which might contribute to the increase of WSSV replication and shrimp mortality.

In conclusion, the full-length cDNA of *Lv*GP was cloned from *L. vannamei*, which shared high identities with the conservative GP family. *Lv*GP transcripts were broadly expressed in most examined tissues with the predominant expression levels in brain and muscle. *Lv*GP transcripts in hepatopancreas and hemocytes could be induced at the early stage after WSSV infection. WSSV replication and shrimp accumulation mortality enhanced after *Lv*GP RNAi. Further study revealed that silencing *Lv*GP transcripts might result in the increase of lactate production to support the energy requirements of virus replication and immune response. However, this metabolic compensation might not be sustainable. Lectin and ALF2 might play a crucial role in *Lv*GP RNAi shrimp defending against WSSV infection, whereas the induction crustin, ALF1 and ALF3 transcripts were inhibited by *Lv*GP RNAi, which might result in the high shrimp mortality after WSSV infection.

Acknowledgements

This research was supported by the Science and Technology Program of Jimei (20172C01), NSFC 41276178 and the Visiting Scholarship from Education Department of Fujian Province for CLY.

References

[1] I.T. Chen, T. Aoki, Y.T. Huang, I. Hirono, T.C. Chen, J.Y. Huang, et al., White spot syndrome virus induces metabolic changes resembling the warburg effect in shrimp hemocytes in the early stage of infection, J. Virol. 85 (24) (2011) 12919–12928.
[2] M.A. Su, Y.T. Huang, I.T. Chen, D.Y. Lee, Y.C. Hsieh, C.Y. Li, et al., An invertebrate Warburg effect: a shrimp virus achieves successful replication by altering the host metabolome via the PI3K-Akt-mTOR pathway, PLoS Pathog. 10 (6) (2014) e1004196.
[3] I.T. Chen, D.Y. Lee, Y.T. Huang, G.H. Kou, H.C. Wang, G.D. Chang, et al., Six hours after infection, the metabolic changes induced by WSSV neutralize the host's oxidative stress defenses, Sci. Rep. 6 (2016) 27732.
[4] T. Watanabe, S. Watanabe, Y. Kawaoka, Cellular networks involved in the influenza virus life cycle, Cell Host Microbe 7 (6) (2010) 427–439.
[5] A.N. Blackford, R.J. Grand, Adenovirus E1B 55-kilodalton protein: multiple roles in viral infection and cell transformation, J. Virol. 83 (9) (2009) 4000–4012.
[6] R.L. Lochmiller, C. Deerenberg, Trade-offs in evolutionary immunology: just what is the cost of immunity? Oikos 88 (1) (2000) 87–98.
[7] N.B. Livanova, N.A. Chebotareva, T.B. Eronina, B.I. Kurganov, Pyridoxal 5'-phosphate as a catalytic and conformational cofactor of muscle glycogen phosphorylase B, Biochemistry (Mosc.) 67 (2002) 1089–1098.
[8] E. Favaro, K. Bensaad, M.G. Chong, D.A. Tennant, D.J. Ferguson, C. Snell, et al., Glucose utilization via glycogen phosphorylase sustains proliferation and prevents premature senescence in cancer cells, Cell Metabol. 16 (2012) 751–764.
[9] P.J. Roach, Glycogen and its metabolism, Curr. Mol. Med. 2 (2002) 101.
[10] J.P. Blass, R.K. Sheu, J.M. Cedarbaum, Energy metabolism in disorders of the nervous system, Rev. Neurol. 144 (1988) 543–563.
[11] C.L. Yao, C.G. Wu, J.H. Xiang, B. Dong, Molecular cloning and response to laminarin stimulation of arginine kinase in haemolymph in Chinese shrimp, *Fenneropenaeus chinensis*, Fish Shellfish Immunol. 19 (2005) 317–329.
[12] C.L. Yao, P.F. Ji, P. Kong, Z.Y. Wang, J.H. Xiang, Arginine kinase from *Litopenaeus vannamei*: cloning, expression and catalytic properties, Fish Shellfish Immunol. 26 (2009) 553–558.
[13] C. Nagai, S. Nagata, H. Nagasawa, Effects of crustacean hyperglycemic hormone (CHH) on the transcript expression of carbohydrate metabolism-related enzyme genes in the kuruma prawn, *Marsupenaeus japonicus*, Gen. Comp. Endocrinol. 172 (2011) 293–304.
[14] N. Zhao, M. Hou, T. Wang, Y. Chen, Y. Lv, Z. Li, et al., Cloning and expression patterns of the brine shrimp (*Artemia sinica*) glycogen phosphorylase (GPase) gene during development and in response to temperature stress, Mol. Biol. Rep. 41 (2014) 9–18.
[15] A. Bhagyalakshmi, P.S. Reddy, R. Ramamurthi, Changes in hemolymph glucose, hepatopancreas glycogen, total carbohydrates, phosphorylase and amino transferases of sumithion-stressed freshwater rice-field crab (*Oziotelphusa senex senex*), Toxicol. Lett. 18 (1983) 277–284.
[16] G. Kamp, H.P. Juretschke, An in vivo 31 P-NMR study of the possible regulation of glycogen phosphorylase a by phosphagen via phosphate in the abdominal muscle of the shrimp *Crangon crangon*, Biochim. Biophys. Acta 929 (1987) 121–127.
[17] W.Y. Hu, C.L. Yao, Molecular and immune response characterizations of a novel AIF and cytochrome c in *Litopenaeus vannamei* defending against WSSV infection, Fish Shellfish Immunol. 56 (2016) 84–95.
[18] F. Vargas-Albores, G. Yepiz-Plascencia, F. Jiménez-Vega, A. Avila-Villa, Structural and functional differences of *Litopenaeus vannamei* crustins, Comp. Biochem. Physiol. B Biochem. Mol. Biol. 138 (2004) 415–422.
[19] K.J. Livak, T.D. Schmittgen, Analysis of relative gene expression data using real-time quantitative PCR and the 2(-Delta Delta C(T)) method, Methods 25 (2001) 402–408.
[20] F. Yang, S.H. Li, F.H. Li, J.H. Xiang, A cuticle protein from the Pacific white shrimp *Litopenaeus vannamei* involved in WSSV infection, Dev. Comp. Immunol. 81 (2018) 303–311.

[21] M.M. Bradford, A rapid and sensitive method for the quantitation of microgram quantities of protein utilizing the principle of protein-dye binding, Anal. Biochem. 72 (1976) 248–254.
[22] S.A. Cruz, Y.C. Tseng, H. Kaiya, P.P. Hwang, Ghrelin affects carbohydrate-glycogen metabolism via insulin inhibition and glucagon stimulation in the zebrafish (Danio rerio) brain, Comp. Biochem. Physiol. Mol. Integr. Physiol. 156 (2010) 190–200.
[23] R. Li, L.N. Zhu, L.Q. Ren, J.Y. Weng, J.S. Sun, Molecular cloning and characterization of glycogen synthase in Eriocheir sinensis, Comp. Biochem. Physiol. B Biochem. Mol. Biol. 214 (2017) 47–56.
[24] J. Duran, J.J. Guinovart, Brain glycogen in health and disease, Mol. Asp. Med. 46 (2015) 70–77.
[25] F. Furukawa, S. Irachi, M. Koyama, O. Baba, H. Akimoto, S.I. Okumura, et al., Changes in glycogen concentration and gene expression levels of glycogen-metabolizing enzymes in muscle and liver of developing masu salmon, Comp. Biochem. Physiol. Part A Molecular & Integrative Physiology 225 (2018) 74.
[26] H. Bacca, A. Huvet, C. Fabioux, J.Y. Daniel, M. Delaporte, S. Pouvreau, et al., Molecular cloning and seasonal expression of oyster glycogen phosphorylase and glycogen synthase genes, Comp. Biochem. Physiol. B Biochem. Mol. Biol. 140 (2005) 635–646.
[27] C.B. Newgard, D.R. Littman, C. van Genderen, M. Smith, R.J. Fletterick, Human brain glycogen phosphorylase. Cloning, sequence analysis, chromosomal mapping, tissue expression, and comparison with the human liver and muscle isozymes, J. Biol. Chem. 263 (1988) 3850.
[28] I. Baranowska-Bosiacka, A. Falkowska, I. Gutowska, M. Gąssowska, A. Kolasa-Wołosiuk, M. Tarnowski, et al., Glycogen metabolism in brain and neurons – astrocytes metabolic cooperation can be altered by pre- and neonatal lead (Pb) exposure, Toxicology 390 (2017) 146–158.
[29] A. Falkowska, I. Gutowska, M. Goschorska, P. Nowacki, D. Chlubek, I. Baranowska-Bosiacka, Energy metabolism of the brain, including the cooperation between astrocytes and neurons, especially in the context of glycogen metabolism, Int. J. Mol. Sci. 16 (2015) 25959–25981.
[30] F. Liu, S.H. Li, G.X. Liu, F.H. Li, Triosephosphate isomerase (TPI) facilitates the replication of WSSV in *Exopalaemon carinicauda*, Dev. Comp. Immunol. 71 (2017) 28–36.
[31] M.L.E. Hernández-Palomares, J.A. Godoy-Lugo, S. Gómez-Jiménez, L.A. Gámez-Alejo, R.M. Ortiz, J.F. Muñoz-Valle, et al., Regulation of lactate dehydrogenase in response to WSSV infection in the shrimp *Litopenaeus vannamei*, Fish Shellfish Immunol. 74 (2018) 401–409 Mar.
[32] G.S. Hotamisligil, E. Erbay, Nutrient sensing and inflammation in metabolic diseases, Nat. Rev. Immunol. 8 (2008) 923–934.
[33] X.Q. Wang, L.L. Wang, H. Zhang, R. Liu, L.S. Song, The carbohydrate metabolism of scallop *Chlamys farreri* in the immune response against acute challenge of *Vibrio anguillarum*, Aquacult. Int. 23 (2015) 1141–1155.
[34] S. Iwanaga, B.L. Lee, Recent advances in the innate immunity of invertebrate animals, J. Biochem. Mol. Biol. 38 (2005) 128–150.
[35] M. Li, C. Ma, H. Li, J. Peng, D. Zeng, X. Chen, et al., Molecular cloning, expression, promoter analysis and functional characterization of a new Crustin from *Litopenaeus vannamei*, Fish Shellfish Immunol. 73 (2018) 42–49.
[36] H. Liu, P. Jiravanichpaisal, I. Söderhäll, L. Cerenius, K. Söderhäll, Antilipopolysaccharide factor interferes with white spot syndrome virus replication in vitro and in vivo in the crayfish *Pacifastacus leniusculus*, J. Virol. 80 (2006) 10365.
[37] M. Li, C.Z. Li, C.X. Ma, H.Y. Li, H.L. Zuo, S.P. Weng, et al., Identification of a C-type lectin with antiviral and antibacterial activity from pacific white shrimp *Litopenaeus vannamei*, Dev. Comp. Immunol. 46 (2014) 231–240.
[38] C.Z. Li, S.P. Weng, J.G. He, WSSV-host interaction: host response and immune evasion, Fish Shellfish Immunol. 84 (2018) 558–571.